Resonance contributions to anti-Stokes/Stokes ratios under surface enhanced Raman scattering conditions

R. C. Maher,[a] J. Hou, and L. F. Cohen
The Blackett Laboratory, Imperial College London, Prince Consort Road, London SW7 2BW, United Kingdom

E. C. Le Ru, J. M. Hadfield, J. E. Harvey, and P. G. Etchegoin[b]
The MacDiarmid Institute for Advanced Materials and Nanotechnology, School of Chemical and Physical Sciences, Victoria University of Wellington, P.O. Box 600, Wellington, New Zealand

F. M. Liu and M. Green
Department of Electrical and Electronic Engineering, Imperial College London, Exhibition Road, .London SW7 2BT, United Kingdom

R. J. C. Brown and M. J. T. Milton
National Physical Laboratory, Hampton Road, TW11 OLW Teddington, Middlesex, United Kingdom

(Received 18 January 2005; accepted 27 June 2005; published online 29 August 2005)

Anti-Stokes/Stokes asymmetries under surface enhanced Raman scattering (SERS) conditions are studied for a wide variety of SERS-active media and different analytes. Evidence is provided for the existence of underlying resonances that create these asymmetries. We show here that these resonances are associated with the electromagnetic coupling between the analyte (probe) and the metal. The work demonstrates the use of the anti-Stokes/Stokes ratio as a tool to understand the hierarchy of resonances in the SERS problem, which is essential for quantification purposes.
 [DOI: 10.1063/1.2004841]

I. INTRODUCTION

A. Overview

Surface enhanced Raman scattering (SERS)[1,2] and some of the offshoot experimental techniques associated with it have the potential to become powerful analytical tools with a wide range of possible applications. An important attraction of SERS, in comparison with the use of fluorescence spectroscopy, is the possibility of combining single molecule (SM) detection with chemical specificity. However, the technique has shown such results with only certain types of molecules (mainly dyes[3–5]) and some types of biomolecules.[6,7] SM detection has been reported for several proteins such as hemoglobin,[8,9] green fluorescent protein,[10] and horseradish peroxidase.[11] Low concentration SERS is of particular interest for potential applications within biomedical spectroscopy,[3,7] where it is widely considered to be a promising new tool. Much work has gone into the characterization of the SERS spectrum of DNA,[6] and since then SERS has been used to identify individual gene segments.[12,13] In addition to its role as a diagnostic tool, SERS may also play a role in the development and understanding of pharmaceutical drugs, in particular in the understanding of how drugs interact with living cells and the environment of organisms.[14,15] Many vitamins, as well as illegal drugs, have also been shown to have well characterized Raman signals that can be amplified via SERS.[16] Understanding the details of the physics of SERS enhancements is therefore of pressing interest for a wide range of applications.

Among other features, anti-Stokes/Stokes ratios have been proposed to be usable for SERS quantification. However, there are several issues associated with the measurement of this ratio that have not yet been clarified;[17–21] it is important accordingly to understand the physical meaning of this ratio in the context of possible applications in quantitative spectroscopy. It has been proposed that the anti-Stokes/Stokes ratio is affected by the various resonances which are present under SERS conditions as well as laser heating.[22] Performing SERS implies carrying out Raman scattering in a medium where several types of resonances may coexist and even interfere with each other. Among them: (i) the single plasmon resonance typical of isolated metallic nano-objects, (ii) collective plasmon resonances produced by interactions among the latter, (iii) direct Raman resonance with the target analyte (in the case of a dye for example), and (iv) coupled plasmon-resonant molecule state (electromagnetic coupling between analyte and metal), etc. All these possible resonances in the problem may affect the intensity of peaks at different wavelengths; the so-called incoming (for the laser) or outgoing (for the scattered photons) Raman resonances. These resonances can affect the Stokes and anti-Stokes intensities differently and can therefore be the source of many of the anomalies reported in the literature.

Very recently,[23] we have observed systematic shifts in anti-Stokes/Stokes ratios with laser wavelength under SERS conditions. These measurements suggest the possibility of establishing a connection between the shifts and the domi-

[a]Electronic mail: Robert.Maher@imperial.ac.uk
[b]Electronic mail: Pablo.Etchegoin@vuw.ac.nz

nant resonant processes. It is the purpose of the present paper to study this effect further, establish its meaning under reproducible enhancement conditions, and summarize the most likely explanations for its existence.

Firstly, we address some particular aspects in more detail to lay the ground work for the subsequent results and discussion.

B. The anti-Stokes/Stokes ratio

In order to discuss the various contributions to the anti-Stokes/Stokes ratio, ρ, we write the most general form of the expression for ρ at low power[3,24]:

$$\rho = \frac{I_{AS}}{I_S} \propto \frac{(\omega_L + \omega_v)^4}{(\omega_L - \omega_v)^4} \exp(-\hbar\omega_v/k_B T) \frac{\sigma_{AS}}{\sigma_S} \sum_{i=1}^{N} \frac{A_{AS}^2}{A_S^2} \qquad (1)$$

where $I_{AS(S)}$ is the intensity of the anti-Stokes (Stokes) Raman mode, $\omega_{L(v)}$ is the frequency of the laser (Raman mode), $\sigma_{AS(S)}$ is the anti-Stokes (Stokes) scattering cross section of the molecule adsorbed to the surface, N is the number of active molecules (not necessarily all molecules in the probe volume), and $A_{AS(S)}$ is the enhancement of the local field at the molecule at the anti-Stokes (Stokes) frequency. The latter term includes both electromagnetic and chemical enhancement effects. In general the enhancement can be site dependent and therefore should be summed over all active sites.

If the scattering cross section and the field enhancement for the anti-Stokes and Stokes modes are the same (for example, under nonresonant conditions), and the ω^4 prefactor can be safely neglected (which is true in most cases because $\omega_v \ll \omega_L$), then we can write

$$\rho = \rho_0 \approx \exp(-\hbar\omega_v/k_B T). \qquad (2)$$

In general however $\rho = \kappa\rho_0$ where κ incorporates all the terms set out in Eq. (1).[25]

C. Potential resonances in the system

For the present study, several resonance conditions have to be scrutinized to understand the possible different Stokes/anti-Stokes scattering conditions. All the samples are composed of metallic nano-objects of different kinds (colloids, pillars, tori, etc). All these structures have a plasmon resonance of their own (as isolated objects) and also coupled resonances through interactions. To this picture we need to add the analyte and its possible contributions to resonances. The main candidates for resonances in the problem are: (i) the direct surface plasmon resonance of the nano-objects in the near ultraviolet (uv) region, (ii) the coupled plasmon-plasmon resonances normally lying somewhere in the visible region,[26] (iii) direct Raman resonance or preresonance with the analyte, and (iv) possible resonances or preresonances with coupled analyte-metal excitations.

Coupled plasmons are important for SERS enhancements potentially contributing to the overwhelming success of SERS under excitation in the red or near infrared region that has been observed in many cases.[27,28] Well defined (broad) coupled plasmon peaks in silver colloids, produced through aggregation, have been studied previously[29] and are widely accepted to exist.

Likewise, the analytes can contribute to the asymmetries between the Stokes and anti-Stokes resonant conditions. Direct resonance in standard Raman scattering is rarely observed for dyes because of the dominance of fluorescence. But the latter can be quenched for dyes in close proximity to metal surfaces due to the existence of rapid nonradiative recombination pathways.[30] Accordingly, the possible observation of a *direct* Raman resonance with the dye cannot be ruled out.

The metal-analyte surface complex is the entity formed when the analyte is physi/chemisorbed onto the surface of the metal, thus affecting the analyte's intrinsic absorption spectrum.[18,31] The interaction can be directly chemical, through the overlap of electronic states of the analyte with the metal, or simply electromagnetic.[31]

We shall address each of these possibilities where appropriate in the following display of results and in the subsequent discussion.

II. EXPERIMENT

SERS experiments have been performed on Ag colloids and two different types of fixed silver substrates. We also used five different types of probes to change the intrinsic role of the analyte. SERS active Ag colloids were prepared by reduction of $AgNO_3$ with sodium citrate (all chemicals purchased from Sigma except where stated), using the procedure described by Lee and Meisel.[32] The colloids produced from this technique have a distribution of sizes with a mean diameter of 60 nm as revealed by dynamic light scattering in solution and scanning electron microscopy (SEM) on dry samples. The particle concentration of the colloids is estimated to be $\approx 10^{12}$ colloids/cm^3. The resulting colloidal suspension is brown-yellowish in appearance and is stable for several months at 4–5 °C.

The second type of SERS active substrates we used were fixed Ag surfaces prepared using island lithography combined with electrodeless plating, as reported elsewhere.[33,34] Using this technique it is possible to fabricate self-assembled arrays of pillars or tori on silicon wafers.[33,34] We have studied SERS anti-Stokes/Stokes ratios from pillars and tori fabricated by this method.[33,34] Tori have, in general, larger enhancement factors compared to pillars under similar experimental conditions, as calculated using adsorption isotherms. A detailed discussion on these substrates and their performance in SERS can be found elsewhere.[33,34]

Of the five analytes used in this study, three play the most important role. SERS active colloidal samples were prepared by mixing 4 mM KCl (activating agent) and 10^{-5} M Rhodamine 6G (RH6G), 10^{-4} M Alexa Flour 488 (AF488, Molecular Probes), or 100 nM 4-(5′-azobenzotriazolyl)naphthalen-1-ylamine (BZT) with the colloids in the ratio 1:1:2, respectively. Both immersion measurements and experiments on dry samples have been performed for these samples. The BZT dye (benzotriazole) was used to evaluate the role of coupled plasmon resonances

in the visible. This latter dye was only used in immersion with colloids. Further details are provided afterwards.

In addition, experiments with pyridine (10^{-2} M and 25 mM KCl on Ag tori) and dithiothreitol (DTT) (10^{-2} M and 4 mM KCl in immersion with Ag colloids) were also performed and will be commented upon when appropriate.

The fixed surfaces (pillars and tori) were prepared for SERS measurements by immersing the surface in a 1:1 solution of either 10^{-5} M RH6G or 10^{-4} M AF488 and 25 mM NaCl (activating agent). The solutions were then allowed to stand for 15 min before measurements were made to allow adsorption of the analyte molecules onto the silver. Measurements were carried out on the fixed surfaces immediately after they had been dried. Absorption spectra of the dyes in solution were measured using a UV-vis spectrometer.

Raman microscopy was performed using a Renishaw 2000 charge-coupled device (CCD) spectrometer equipped with an Olympus BH-2 confocal microscope using different laser lines from either an Ar^+, HeNe, or infrared diode lasers as excitations. Low laser intensities in the range 0.5–1.0 mW were used to avoid heating/pumping effects, for both the wet and dry measurements.[23] SERS spectra were obtained from colloidal solutions using a $\times 60$ immersion objective index matched to water. Heating effects occurring within the colloidal suspension due to the laser are further minimized by diffusion. SERS measurements on the dried samples were made using a $\times 50$ objective. The beam width was approximately 1.5 μm. Intensities within 250 cm^{-1} of the laser were distorted by the notch filter rendering peaks within this region unusable for the determination of anti-Stokes/Stokes ratios.

Data were recorded with integration times in the range of 30–120 s and with 10 to 30 accumulations depending on the specific sample. Due to the large concentrations, integration times, and the scattering volume involved in measurements on the colloidal solutions, each measurement represents a spatial average over many scattering geometries representative of the different samples. Ten or more measurements were made on the dried surfaces at different locations to investigate the effect, if any, of local geometry changes on the ratios and to gain an average over scattering geometries. The Raman peaks were then analyzed using standard Voigt functions with subtracted backgrounds (Peakfit and Origin).

It is important to ensure that the experimentally determined values of the ratios (ρ) are physically meaningful and do not represent the wavelength sensitivity of the optical layout and detector. We calibrated our system using ratios calculated from known organic compounds with many Raman active lines under non-SERS conditions. We used the dye $TPPS_4$ and β-carotene to calibrate the response of the system (see Fig. 1 in Ref. 23). The ρ was calculated for all visible peaks and these were compared to the theoretical values. This allowed us to obtain calibration curves which assure us there is no spectral artifacts from the collecting optics, notch filter, grating, or CCD in the reported values.

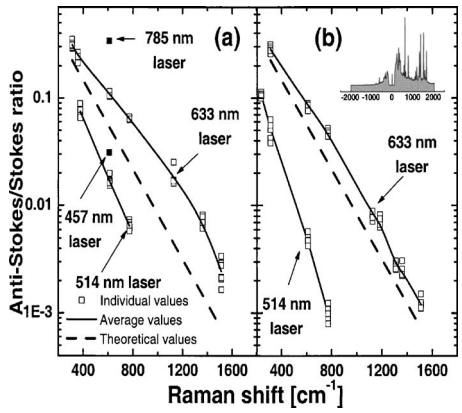

FIG. 1. Anti-Stokes/Stokes ratio measured with four different excitation wavelengths (457, 514, 633, and 785 nm) for: (a) an aqueous solution of RH6G mixed with Ag colloids and KCl as activating agent (as described in the text), and (b) a dry sample. These measurements were made at low excitation intensity to avoid any possible heating or pumping effects. The solid line in both cases is the theoretical value at room temperature from Eq. (2). Note that intensities are on a log scale. A systematic (upward) downward shift is observed for all the observable modes for the (633) 514 nm laser. The inset in (b) shows a typical SERS spectrum of RH6G in these measurements. Intensities within 250 cm^{-1} of the laser are distorted by the notch filter. Measurements for 785 and 457 nm lasers are only performed for the 610 cm^{-1} mode of RH6G in immersion. See the text for further details.

III. RESULTS

A. Colloids in solution or dry

We examine first RH6G with colloidal silver. Figure 1 shows the anti-Stokes/Stokes ratio of RH6G under SERS conditions with colloidal silver in both solution and dried samples for 457, 514, 633, and 785 nm laser excitation. Figure 1 shows a well defined and reproducible trend. The results on the left are from immersion measurements and those on the right are from the dried samples. The Raman spectrum of RH6G is shown as an inset in Fig. 1(a). The dashed line gives the theoretical ratio value. The anti-Stokes/Stokes (aS/S) ratio (for visible modes in the spectrum) measured for the 514 nm laser is lower than the theoretical ratio, while it is increased for 633 nm excitation. The difference in resonance conditions for the anti-Stokes and Stokes fields become less important for smaller Raman shift, because the difference in (absolute) energy between the two decreases. Hence, as the modes approach the laser energy, ρ approaches the theoretical value, as expected.

Measurements with the 457 and 785 nm lasers were made in solution for one mode only. These measurements help to improve our knowledge of the hidden resonance profile affecting this ratio. The 457 nm ratio is suppressed with respect to the theoretical value but to a lesser extent than the 514 nm result. In the case of the ratios measured with the 785 nm laser, these are further increased from the theoretical value than those measured with the 633 nm laser. The challenge is now to build up an understanding of the resonance profile that may be the source of the anomalous ratio. We would like to stress that, besides any possible uncertainties in the interpretation of the origin of these resonances, the data are extremely robust and similar results have been obtained over many different batches of samples and, in addition, using another spectrometer (LabRam from Jobin Yvon).

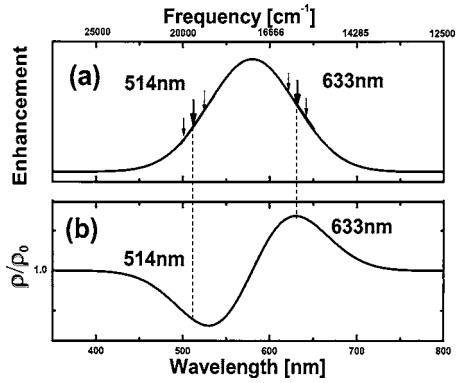

FIG. 2. (a) Schematic view of a typical enhancement profile associated with a resonance in the system. The arrows indicate the position of the 514 nm and 633 nm lasers and the anti-Stokes and Stokes signal for a particular mode. (b) The deviation for a particular mode of the aS/S ratio over the theoretical value as a result of the presence of the resonance shown in (a).

A possible scenario for an underlying resonance that would reproduce these results is displayed schematically in Fig. 2(a). If a resonance is broad enough to span the entire visible range, the window spanned by the Raman signals is a relatively small region around the laser on the scale of the entire visible range. Accordingly, the gradient of the resonance profile gives, in a first approximation, an indication of whether the ratio will lie above or below the theoretical value. For lasers above the maximum of the resonance in energy the aS/S ratio will be depressed, while those below in energy will be increased. This is illustrated in Fig. 2(b). On top of this general underlying trend, variations for different modes indicate the local dispersion of the resonance around a specific laser energy; dispersion effects are expected to be more important the larger the Raman shift with respect to the laser. This technique can be used to map out the shape of the underlying resonance if one particular resonance effect dominates. Note that there is no general rule that makes the wavelength dependence of the absorption spectrum exactly equal to that of the SERS enhancement of the complex system. In fact, they can be quite different,[35] not least because the Raman process is inherently more complex as it also involves the scattered photon.

A resonance, such as that observed in Fig. 2, which is in the spectral energy range spanning the green-red region, is anticipated for coupled plasmons[36] (which are geometrically determined), or coupled plasmon-dye resonances as we shall show later. But also a direct resonance or preresonance with the dye cannot be ruled out at this stage. Note that there are subtle differences between the colloids in solution and dried that reflect changes in the hidden resonance dispersion due to either different statistical averaging effects or the different nature of the coupled-plasmon resonance.

The first question we address is: What is the effect of the geometry? It is well known that coupled plasmon resonances are very geometry dependent. It seems surprising in that respect that colloids in solution produce results which are qualitatively very similar to aggregated dried colloids, as shown in Figs. 1(a) and 1(b).

Hence, in order to identify if this hidden resonance is predominantly determined by geometry we move to a study of the same analyte but using a very different SERS active medium, with a radically different geometry.

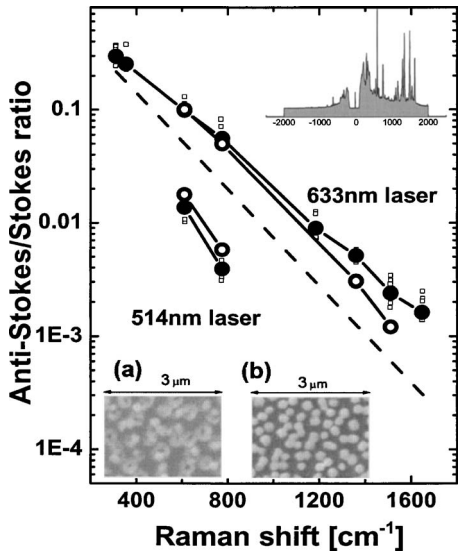

FIG. 3. Anti-Stokes/Stokes ratios measured with two different excitation wavelengths for RH6G mixed with activating agent (NaCl) and dried onto the two different surfaces described in the text [Ag tori (open circles) and pillars (full circles) (Refs. 33 and 34)]. SEM images of the structures with a relevant length scale are shown in the insets at the bottom of the figure: (a) toroids and (b) pillars. Low excitation intensities were also used here to minimize any possible heating/pumping. As in Fig. 1, the dashed line is the calculated theoretical ratio from the thermal population. The same systematic shifts in the ratios seen on colloids are observed on these substrates with markedly different coupled plasmon resonances.

B. Ag tori and pillars

To investigate this next step, we performed the same anti-Stokes/Stokes ratio experiments on Ag pillars and tori that make up fixed SERS surfaces with reproducible enhancements, as described in Refs. 33 and 34. Measurements made with the 514 nm laser were restricted by the strong fluorescence of RH6G. The anti-Stokes intensity is small in these samples compared to that of the colloids, with a substantial amount of photobleaching occurring during the integration time of the experiment, even for very low incident powers. These factors combine to make it difficult to obtain both the anti-Stokes and the Stokes intensities for most modes except two. These problems are avoided when using the 633 nm excitation, as this is far away from the direct absorption of RH6G and the signal is typically more stable.

Figure 3 shows the anti-Stokes/Stokes ratio for RH6G measured on both Ag pillars and tori. As before, measurements were taken at low incident powers to avoid any possible contributions from heating or pumping. The individual measurements are shown in Fig. 3 as small open squares, and give an idea of the spread in the data, which are larger than in colloidal samples. We interpret the increase in spread as the manifestation of larger (relative) changes in local geometry in these dried samples. Nevertheless, the results show that, in general terms, the average ratio measured on these

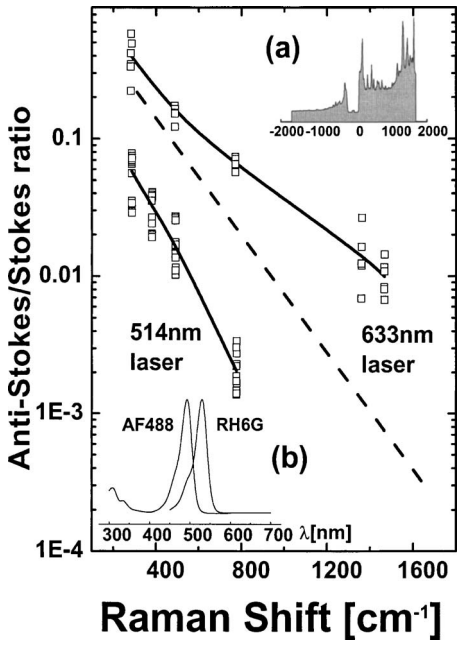

FIG. 4. Anti-Stokes/Stokes ratio ρ measured with two different excitation wavelengths on a dried Ag-colloid cluster with AF488 and activating agent as described in the text. The spectrum of this dye is shown in inset (a), and the absorption spectra of both AF488 and RH6G are shown in inset (b). Even though the direct outgoing resonance with the dye should be different from RH6G, this dye shows exactly the same shifts in the anti-Stokes/Stokes ratios as before. A direct resonant effect with the dye cannot explain the observed asymmetries in the ratios. See the text for further details.

surfaces is very similar to those obtained from colloidal samples. As before, this effect is robust and reproducible over many different batches of samples.

From these experiments we learn that the postulated hidden resonance affecting the anti-Stokes/Stokes ratios (Fig. 2) does not appear to be strongly controlled by geometry for this analyte. Admittedly, coupled plasmon resonances are broad in nature and, accordingly, a simple problem of lack of sensitivity to the overall changes in their dispersion cannot be ruled out. But coupled plasmons in aggregated colloids are expected to be *very* different from their equivalents in solution and, in turn, very different to coupled plasmons in tori and pillars which are much larger in size for a start and have completely different average topological features.[33,34] The experimental result seems to be certainly very robust compared to expected changes.

This suggests that the underlying resonance should be connected more to the presence of the analyte itself or to the interaction between the analyte and Ag on a very local scale.

In order to explore whether the direct resonance with the dye is important we look at the effect of two different dyes, namely: Alexa Fluor 488 (AF488, from Molecular Probes) and the recently synthesized[37] SERS-active benzotriazole dye (BZT) described in the experimental section.

C. Direct resonance with dye molecules

The analyte AF488 was prepared with 4 mM KCl and Ag colloids and dried onto a glass slide. To compare with the previous case of RH6G, absorption spectra for both RH6G and AF488 are provided in Fig. 4(b). This shows that there is a significant change in the resonance profile for the two dyes. This means that if a direct resonance with the dye is playing a dominant role, measurements with the 514 nm laser should produce very different results for RH6G and AF488 in terms of a direct resonance effect. Figure 4 shows the experimentally determined ratios for both 514 and 633 nm lasers, along with the theoretically expected values (dashed line) for AF488. The squares are the individual measurements and the solid lines are average ratios. As with RH6G, AF488 shows ratios which are above the expected theoretical values for 633 nm excitation. The surprising result is that the ratios calculated for the 514 nm laser are again below the theoretical value; a situation similar to the RH6G case.

If direct resonance or pre-resonance with the dye had been the dominant effect to explain the observed anti-Stokes/Stokes asymmetry, the AF488 data should have provided a clear-cut difference for the 514 nm laser. In this case, both lasers lie below the absorption edge of the dye and, accordingly, both aS/S ratios should be above the theoretical one, albeit by different extents. This is not what it is observed experimentally and indicates that the underlying resonance producing the asymmetry in the ratio must have a different origin.

Finally, Fig. 5 shows the aS/S-ratio results for BZT. This dye has the maximum of the absorption further into the deep-blue/near-UV region at 400 nm. For this latter dye, we do finally see a change in the aS/S ratios with respect to the other analytes. The 514 nm laser data are still below the expected theoretical ratio while the results for 633 nm excitation are only marginally anomalous in this latter case. The results in this subsection thus indicate that the analyte is indeed related to the underlying resonance producing the aS/S-ratio asymmetries, but in a way which is not *directly* related to the absorption spectrum of the dye. The next subsection is devoted to a plausible simple explanation of these observed phenomena.

D. Coupled plasmon-analyte resonance

One explanation of the experimental observations is to invoke an underlying resonance produced by a coupled-plasmon-analyte interaction. We explore this possibility here.

The problem of the coupling between a dipolar resonant optical absorption and a close metallic surface has been studied in the past in various approximations. We follow the treatment of the coupled plasmon-dye resonance model of Fuchs and Barrera in Ref. 31; details are reduced to a minimum here. If we ignore the problem of nonlocality and concentrate on the local response only (also treated by King *et al.*[38]) (the dielectric response of the metal does not depend on the wavevector of the light), it is possible to study qualitatively how the resonant profile of a dye would be affected by the close proximity of the metal. By close proximity we mean here distances of the order of the molecular size itself ($\sim$1 nm or smaller). The experimental evidence suggests that, to a first approximation, the enhancement process can be separated into different contributions, as far as the wavelength dependence is concerned. When we look at the interaction of the molecule with the local field, the dipole

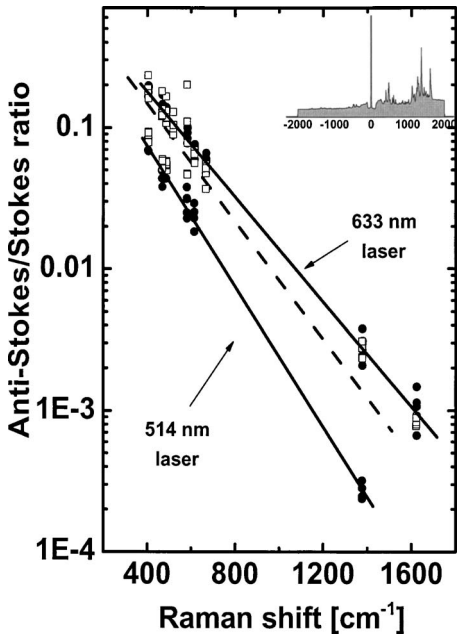

FIG. 5. Anti-Stokes/Stokes ratio ρ measured with two different excitation wavelengths for BZT. Results for different enhancing media are displayed (open symbols: colloids, full symbols: pillars) and the theoretical values are again indicated by a dashed line. The Raman spectrum of this dye is shown schematically in the inset. The absorption of BZT is centered at 400 nm and has a full width at half maximum of 200 nm. This dye shows a slightly different result with respect to the previous ones: the aS/S values for 633 nm excitation are only marginally above the theoretical expectation, while the 514 nm laser is still below. See the text for further details.

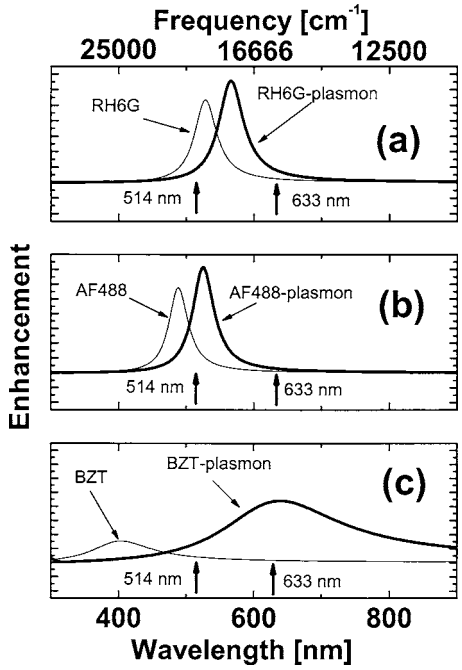

FIG. 6. Modified absorption spectra for three model dielectric functions for RH6G (a), AF488 (b) and BZT (c) which result from the formation of the metal-analyte surface complex. These shifts have been calculated using the model in Ref. 31 and appropriate models for the optical properties of the different dyes. The resonance with the dye-metal coupled plasmon does not follow linearly the change in the absorption maximum of the dye because of the coupling (anticrossing) with the surface plasmon of the metal. As a result, dyes like like RH6G and AF488 are left in very similar resonant conditions with the 514 and 633 nm laser lines being on opposite sides of the resonance profile. BZT is a smaller molecule and has a wider absorption spectrum centered at 400 nm; its coupled dye-plasmon resonance leaves both lasers in a different situation when compared to RH6G and AF488. See the text and Ref. 31 for further details.

transition of the dye can be changed by the close presence of a dielectric surface. The interaction of the dipole with a flat surface will be a good approximation as far as the surface is "flat" on length scales comparable to the molecular size ($\sim$1 nm). This is expected to be the case in most situations (including the present case) except when very sharp topological features of the order of a fraction of a nanometer exist. The (local) dielectric function of Ag can be reasonably well represented by an analytic Drude model with parameters provided in Ref. 26. Furthermore, an analytic model for the optical properties of RH6G can be obtained from Ref. 39. The optical properties of AF488 (having a core structure very similar to RH6G) can be modelled with the same overall parameters of of RH6G, except for the maximum of the absorption which is shifted from 528 nm for RH6G (Ref. 39) to 488 nm for AF488. There are no analytic models available for the optical properties of BZT, but a reasonable fit to our own experimental data of the absorption spectrum in Fig. 5 can be obtained by assuming the maximum of the absorption to be at 400 nm and using a much wider FWHM as compared to RH6G and AF488. Note that the maximum of the absorption of BZT is reported to be at 435 nm in Ref. 37; the difference with our experimental data is most likely produced by the fact that we are using a different solvent (water). Assuming a $\sim$1 nm average separation with respect to the metal for RH6G and AF488 and a slightly smaller value ($\sim$0.65 nm) for BZT (accounting for the different relative sizes of both families of molecules) we can compute the plasmon-dye resonance profile with the model in Ref. 31.

Figure 6 is a triple plot showing the expected coupled plasmon-analyte resonance for the three cases presented so far: RH6G, AF488, and BZT. The model shows that the coupled resonance is less sensitive to a blueshift in the absorption of the analyte because it is actually anticrossing with the intrinsic surface plasmon resonance of the metal and it is *held back* in the interaction. Therefore, a change from 528 to 488 nm, as in the case of RH6G and AF488, results in a coupled resonance that still has the 514 and 633 nm lasers on opposite sides of the maximum in both cases, as shown in Figs. 6(a) and 6(b). For BZT the situation is different; the combination of the smaller overall size of the molecule and a broader absorption peak around 400 nm results, after the interaction with the metal is included, in a peak which is pushed further down towards the red. A combination of the experimental data in Fig. 5 and the schematic plot in Fig. 2 suggests, in fact, that the 514 nm laser should be located on the left of the maximum of the coupled resonance, while the 633 nm laser would be somewhere close to the maximum where ΔR in Fig. 2(b) is small. The details are obviously not *exactly* reproduced in Fig. 6(c) for BZT due to the limitations of the analytic model we are using for this dye and the intrinsic approximations of the coupled dye-plasmon model.[31] But despite this limitation, it is quite clear that a model based on a coupled metal analyte resonance can, in principle, explain very easily apparent contradictions in the resonance profiles, and in addition the insensitivity to geometry.

The results in this subsection combined the phenomenology of the dye-plasmon coupled model[31] suggest that only SERS active probes with intrinsic resonances further into the UV (above the single plasmon resonance of the metal) should be able to overcome the interaction effect and become less sensitive to aS/S asymmetries. This interpretation also suggests that a direct effect of the coupled plasmons is not playing a dominant role in the asymmetry between aS/S ratios for lasers in the visible, at the analyte concentration we have used here.

We explore the role of the intrinsic resonance of analytes with gaps further in the UV in the next subsection; this is to support the interpretation of the probe being involved in the origin of the asymmetries.

E. Nonresonant molecules

We provide two examples of probes with intrinsic resonances in the deep-UV region for the sake of completeness. The two molecules studied here are pyridine (Py) and dithiothreitol (DTT). Pyridine was dissolved in deionized water to a concentration of 10^{-2} M. This was then mixed in a ratio of 50:50 with 25 mM KCl. A substrate with fixed Ag toroidal features was then immersed in the final solution and left for 15 min to allow adsorption on to the surface. SERS measurements were made by focusing onto the surface of the sample through a thin layer of liquid with a long working distance $\times 50$ objective. DTT was dissolved in deionized water to a concentration of 10^{-2} M which was then mixed in a ratio of 50:50 with 4 mM KCl. The resulting solution was then mixed in a ratio of 50:50 with Ag colloids. A small amount was dried onto the surface of a glass slide and SERS measurements were made with a $\times 50$ short working distance objective on the colloidal clusters which were formed. All measurements were made at low laser powers.

Figures 7(a) and 7(b) shows the results of these two molecules. Both Py and DTT have a large spread in data. Both of these molecules have comparatively modest SERS enhancements with respect to the dyes presented in the previous subsections. Despite the spread in the data, it is clear from the figure that these molecules present aS/S asymmetries which are compatible with the theoretical expectation. This result is again robust and reproducible over many different batches of samples. The coupled analyte-plasmon model of the previous section predicts in this case negligible asymmetries for aS/S ratios for these molecules. In our opinion, these final observations show that the aS/S ratio is controlled to a large degree by an underlying resonance which is most likely a coupling between the dye and the metal.

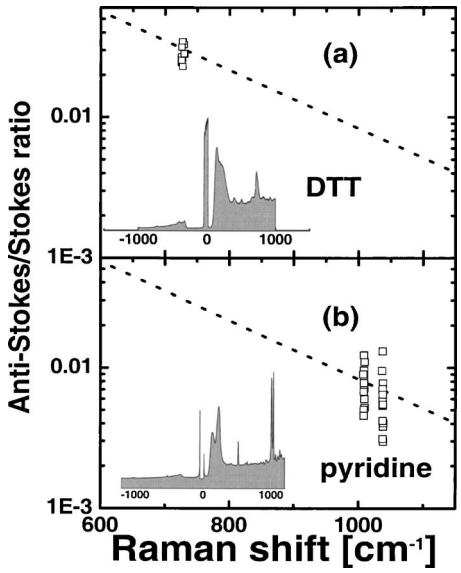

FIG. 7. Anti-Stokes/Stokes ratio ρ measured with the 633 nm laser for the nonresonant molecules (a) DTT and (b) pyridine. The measurement in (a) was made on a sample of DTT mixed with activating agent and Ag colloid which was dried. The pyridine measurement was made on a fixed Ag surface of toroids with activating agent. Although there is a relatively large spread in the data, the average ratio for both molecules agrees well with that theoretically predicted. These results suggest that the further into the UV region the intrinsic resonance of the dye is, the less affected the aS/S ratio in the visible. It also rules out a strong influence from coupled plasmons in the observed asymmetries.

IV. CONCLUSIONS

SERS is a problem where a hierarchy of optical resonances may play competing roles. In metallic disordered structures, like colloidal aggregates, a wide distribution of resonances is expected though the visible range due to coupled plasmons. This primary resonance, which is needed to explain the huge electromagnetic enhancements frequently observed under SERS conditions at low analyte concentrations should have a contribution to asymmetries between Stokes and anti-Stokes intensities for a given excitation. But, in addition, other resonance effects can *modulate* the overall enhancement. In this paper we have shown evidence for the latter. We have shown that systematic shifts in the anti-Stokes/Stokes ratio as a function of laser wavelength exist for a wide variety of metallic nanostructured SERS media. These range from colloidal solutions to dried fixed silver tori and pillars. It is difficult then to make a direct connection with topological differences, and the corresponding distributions of coupled plasmons, in these samples. The asymmetries seem to be related to the only common feature among these samples which is the presence of the same metal and the same analyte. We then expect the behavior to depend on the characteristics of the analyte. We showed that this is, in fact, the case; but the changes cannot be directly linked to a direct resonance with the probe itself. It is only when we invoke a coupled dye-plasmon resonance that these apparent contradictions are resolved. We did so by using a well established electromagnetic coupling model between a probe and a metal surface developed in Ref. 31. In this paper we have shown that the interaction of the dipole with a "flat" surface is a good approximation to understand qualitatively several experimental facts. More work needs to be done to prove this in general.

We also show in this paper that the anti-Stokes/Stokes ratio as a function of excitation frequency can be used to map the optical properties of the underlying collective resonances of various SERS active media with different ranges of analytes. The results in this paper suggest that the use of

tunable lasers with aS/S-ratio studies should be particularly useful to map the resonant interaction between the probes and the metal.

ACKNOWLEDGMENTS

P.G.E., L.F.C., F.M.L., and M.G. acknowledge partial support for this work by the Engineering and Physical Sciences Research Council (EPSRC) of the UK under Grants No. EPSRC-UK GR/R28775 and No. EPSRC-UK GR/T06124. R.C.M. acknowledges partial support from the National Physical Laboratory (NPL) in the U.K. The authors are indebted to Peter Kollensperger (Imperial College) for providing a sample of DTT for use in these experiments.

[1] M. Moskovits, Rev. Mod. Phys. **57**, 783 (1985).
[2] A. Otto, in *Light Scattering in Solids*, edited by M. Cardona and G. Güntherodt (Springer, Berlin, 1984), p. 289.
[3] K. Kneipp, H. Kneipp, I. Itzkan, R. R. Dasari, and M. S. Feld, J. Phys.: Condens. Matter **14**, R597 (2002).
[4] K. Kneipp, H. Kneipp, I. Itzkan, R. R. Dasari, and M. S. Feld, Chem. Phys. **247**, 155 (1999).
[5] K. Kneipp, H. Kneipp, G. Deinum, I. Itzkan, R. R. Dasari, and M. S. Feld, Appl. Spectrosc. **52**, 175 (1998).
[6] K. Kneipp, H. Kneipp, V. B. Kartha, R. Manoharan, G. Deinum, I. Itzkan, R. R. Dasari, and M. S. Feld, Phys. Rev. E **57**, R6281 (1998).
[7] T. Vo-Dinh, L. R. Allain, and D. L. Stokes, J. Raman Spectrosc. **33**, 511 (2002).
[8] H. Xu, E. J. Bjerneld, and M. Käll, Phys. Rev. Lett. **83**, 4357 (1999).
[9] P. Etchegoin, H. Liem, R. C. Maher, L. F. Cohen, R. J. C. Brown, M. J. T. Milton, and J. C. Gallop, Chem. Phys. Lett. **367**, 223 (2003).
[10] S. Habuchi, M. Cotlet, R. Gronheid, G. Dirix, J. Michiels, J. Vanderleyden, F. C. De Schryver, and J. Hofkens, J. Am. Chem. Soc. **125**, 8446 (2003).
[11] E. J. Bjerneld, Z. Foldes-Papp, M. Käll, and R. Rigler, J. Phys. Chem. B **106**, 1213 (2002).
[12] M. Culha, D. Stokes, L. R. Allain, and T. Vo-Dinh, Anal. Chem. **75**, 6196 (2003).
[13] M. Culha, D. Stokes, and R. Vo-Dinh, Expert Rev. Mol. Diagn. 3, 669 (2003).
[14] G. Breuzard, J. F. Angiboust, P. Jeannesson, M. Manfait, and J. M. Millot, Biochem. Biophys. Res. Commun. **320**, 615 (2004).
[15] G. Fabriciova, S. Sanchez-Cortes, J. V. Garcia-Ramos, and P. Miskovsky, Biopolymers **74**, 125 (2004).
[16] S. C. Pinzaru, I. Pavel, N. Leopold, and W. Kiefer, J. Raman Spectrosc. **35**, 338 (2004).
[17] K. Kneipp, Y. Wang, H. Kneipp *et al.*, Phys. Rev. Lett. **76**, 2444 (1996).
[18] T. L. Haslett, L. Tay, and M. Moskovits, J. Chem. Phys. **113**, 1641 (2000).
[19] R. C. Maher, M. Dalley, E. C. Le Ru, L. F. Cohen, P. Etchegoin, H. Hartigan, R. J. C. Brown, M. J. T. Milton, and J. C. Gallop, J. Chem. Phys. **121**, 8901 (2004).
[20] A. Otto, J. Raman Spectrosc. **33**, 593 (2002).
[21] Y. Maruyama, M. Ishikawa, and M. Futamata, J. Phys. Chem. B **108**, 673 (2004).
[22] A. G. Brolo, A. C. Sanderson, and A. P. Smith, Phys. Rev. B **69**, 045424 (2004).
[23] R. C. Maher, L. F. Cohen, P. Etchegoin, H. J. N. Hartigan, R. J. C. Brown, and M. J. T. Milton, J. Chem. Phys. **120**, 11746 (2004).
[24] H. Xu, J. Aizpurua, M. Käll, and P. Apell, Phys. Rev. E **62**, 4318 (2000).
[25] M. Cardona, in *Light Scattering in Solids II* (Springer, Berlin, 1990).
[26] R. Rojas V and F. Claro, J. Chem. Phys. **98**, 998 (1993).
[27] P. Etchegoin, L. F. Cohen, H. Hartigan, R. J. C. Brown, M. J. T. Milton, and J. C. Gallop, J. Chem. Phys. **119**, 5281 (2003).
[28] E. Prodan, C. Radloff, N. J. Halas, and P. Nordlander, Science **302**, 419 (2003).
[29] N. Félidj, J. Aubard, and G. Levi, J. Chem. Phys. **111**, 1195 (1999).
[30] I. A. Larkin, M. I. Stockman, M. Achermann, and V. I. Klinov, Phys. Rev. B **69**, 121403 (2004).
[31] R. Fuchs and R. G. Barrera, Phys. Rev. B **24**, 2940 (1981).
[32] P. C. Lee and D. Meisel, J. Phys. Chem. **86**, 3391 (1982).
[33] M. Green and F. M. Liu, J. Phys. Chem. B **107**, 13015 (2003).
[34] F. M. Liu and M. Green, J. Mater. Chem. **14**, 1526 (2004).
[35] P. Etchegoin, R. C. Maher, E. C. Le Ru, and L. F. Cohen, J. Phys. (preprint).
[36] K. Faulds, R. E. Littleford, D. Graham, G. Dent, and W. E. Smith, Anal. Chem. **76**, 592 (2004).
[37] D. Graham, C. McLaughlin, G. McAnally, J. C. Jones, P. C. White, and W. E. Smith, Chem. Commun. (Cambridge) **11**, 1187 (1998).
[38] F. W. King, R. P. Van Duyne, and G. C. Schatz, J. Chem. Phys. **69**, 4472 (1978).
[39] H. Xu and M. Käll, Phys. Rev. Lett. **89**, 246802 (2002).